ROMANIAN JOURNAL OF INFORMATION SCIENCE AND TECHNOLOGY
Volume **14**, Number 4, 2011, 334–345

Analysis of GaN Based SAW Resonators including FEM Modeling

A. ŞTEFĂNESCU[1], D. NECULOIU[1], A. MÜLLER[1],
A. DINESCU[1], G. KONSTANTINIDIS[2], A. STAVRINIDIS[2]

[1]IMT Bucharest, 126A (32B), Erou Iancu Nicolae str.,
077190 Bucharest, Romania
E-mail: alexandra.stefanescu@imt.ro

[2]FORTH-IESL-MRG Heraklion,
PO Box 1527, Crete, Greece
E-mail: aek@physics.uoc.gr

Abstract. This paper proposes an analysis of two types of Surface Acoustic Wave (SAW) resonators composed of interdigital transducers (IDT) of 200 nm wide on GaN/Si devoted for GHz applications. Two finite element (FEM) models for basic periodic cells are given to demonstrate de characteristics of the resonators at different resonance frequencies. E-beam lithographical techniques have been used for the IDT fingers. Experimental measurements of the S parameters have shown a good agreement with the simulation results regarding the resonance frequency.

Keywords: surface acoustic wave resonator (SAW), finite element simulation (FEM), e-beam lithography.

1. Introduction

Surface acoustic wave devices have been used intensively for the fabrication of high performance filters with applications in communication systems (mobile phones, wireless local area networks) [1, 2]. Recently sensor technology has grown rapidly and SAWs have been explored for the fabrication of very sensitive gas [3] or humidity sensors [4].

The development of semiconductor based acoustic devices working at frequencies higher than 2 GHz was determined by the progress in manufacturing high quality

piezoelectric semiconductor layers like AlN and GaN on sapphire, diamond, and, more recently, on high-resistivity silicon. Gallium Nitride (GaN) is of great technological interest for the monolithic integration with other passive and active circuit elements. GaN has become a very promising substrate material for the SAW devices due to its high quality properties: high acoustic wave velocity, electromechanical coupling and thermal stability [5]. Lately, a considerable attention has been paid to GaN layers grown by metalorganic chemical vapour phase deposition (MOCVD) on Silicon [6], [7], [8]. Recently the first SAW structures manufactured on GaN/Si working beyond 5 GHz have been reported [9].

Many theoretical analytical methods have been developed for simulating SAW devices: coupling of modes (COM), equivalent circuit models or delta function model. In order to develop a very accurate model that can be further incorporated in a more complex device, numerical simulations must be employed. Finite element analysis is a good choice because it is based on solving differential equations, where the device characteristics are obtained based on material properties, regardless of device structure [10]. Commercial software based on finite element method (FEM) such as COMSOL Multiphysics or ANSYS can accurately model piezoelectric structures in frequency domain [10, 11, 12, 13].

In case of two ports SAW resonators, surface acoustic waves propagated at the surface of a piezoelectric material are generated by applying a voltage to the input interdigital transducer (IDT). In this paper two types of transducer configurations (single – electrode transducer and split electrode transducer) will be analysed. The general purpose of this paper is to present the numerical modeling of SAW resonators on GaN/Si realized based on nanolithography techniques with a central frequency in GHz range. Details on the theoretical background are given in Section 2 and the modeling procedure based on finite element method is presented in Section 3. Section 4 discusses the fabrication and characterization of the SAW devices. Based on the results presented, in Section 5 conclusions are drawn.

2. Theoretical background

SAW resonators often consist of up to hundred of electrodes that can be about 100 times longer than wide. Therefore, the edge effects are negligible and the resonator can be regarded as an infinitely extended periodic structure [14, 15]. The model geometry can be reduced to one unit cell as shown in Fig. 1. This periodicity is advantageous for the numerical model as sometimes is impossible to simulate the entire structure and this method reduces tremendously the simulation time. Moreover, from a basic periodic cell we can obtain essential information on the frequency characteristic and on the surface acoustic mode shapes.

In this paper, two types of SAW structures are investigated: A – the classical single electrode transducer (Fig. 1 left) and B – split electrode transducer (Fig. 1 right).

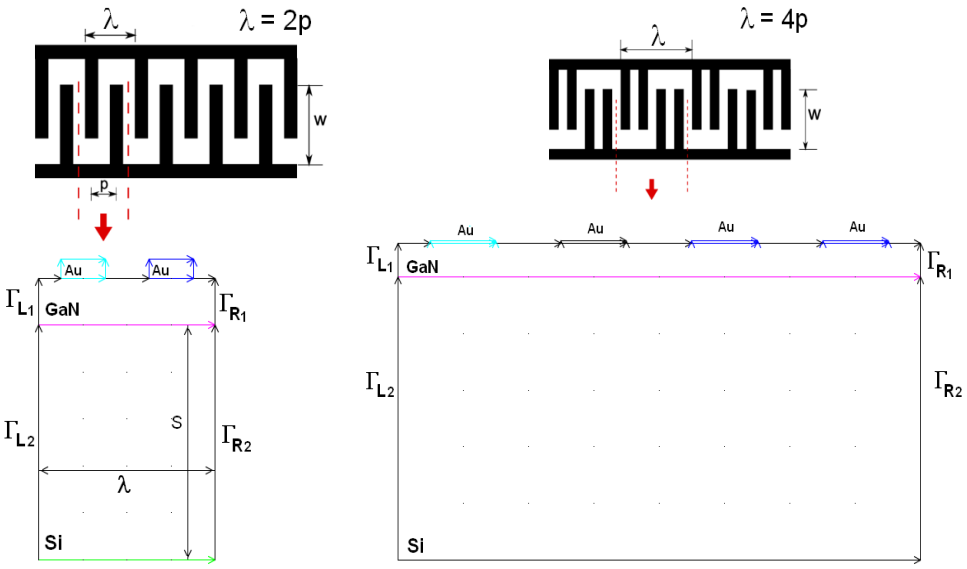

Fig. 1. Model geometry of structures A and B (one periodic cell as employed in the simulation).

The advantage of double electrode transducers is that they are non – reflective while the single electrode transducers are reflective [16]. The disadvantage of this type of transducer is the reduction of the electrode pitch (p) which limits the operating frequency to half. So the wavelength (λ) is calculated as:

$$\lambda = 2 \times p = 2 \times 0.4 \text{ μm} = 0.8 \text{ μm} \tag{1}$$

in case of structure A, and for structure B as in (2):

$$\lambda = 4 \times p = 4 \times 0.4 \text{ μm} = 1.6 \text{ μm}. \tag{2}$$

The central frequency (f_0) can be easily obtained analytically for both cases [17] from relation (3):

$$\nu = \lambda \times f_0, \tag{3}$$

where ν is the acoustic velocity of the piezoelectric layer.

3. Finite element modeling

The proposed structures (A and B) have been investigated with finite element software COMSOL Multiphysics (MEMS module) [18] and the results have been compared. The surface acoustic waves make use of the piezoelectricity in order to propagate. The Piezo Plane Strain application mode from MEMS module is dedicated to model the piezoelectricity and computes the global displacements (u, v) in

the x and y directions and the electric potential (V) in a state of plane strain. These dependent variables represent the degrees of freedom. The piezoelectric constitutive equations give the relation between the stress, strain, electric field and electric displacement:

$$\mathbf{T} = c_E\mathbf{S} - e^T\mathbf{E}, \tag{4}$$

$$\mathbf{D} = e\mathbf{S} + \varepsilon_S\mathbf{E}, \tag{5}$$

where $\mathbf{T}$ represents the stress matrix, $\mathbf{S}$ the strain matrix, $\mathbf{E}$ [V/m] the electric field, $\mathbf{D}$ the electric displacement matrix [C/m^2], c_E is the elasticity matrix [Pa], e^T is the piezoelectric matrix [C/m^2] and ε_S is the permittivity matrix.

The proposed modeling of the SAW structures is fairly simple as it is reduced to the analysis of a single unit cell. An alternating voltage is applied on the electrodes to determine the frequency response of the device: for structure A (Fig. 1 left), the unit cell has two electrodes, one grounded and one has 1 V input voltage and for structure B (Fig. 1 right), the unit cell has four electrodes, 2 grounded and two assigned with a polarization voltage of 1 V.

In both cases, a piezoelectric GaN layer of 1.2 μm has been used for simulations. IDT Au electrodes 80 nm thick and 200 nm wide have been considered. Details on the material parameters used in the simulations are given in Table 1 [19].

The modeling of one wavelength of the SAW device is possible only if periodic boundary conditions ($\Gamma_{L1}, \Gamma_{L2}, \Gamma_{R1}, \Gamma_{R2}$) are applied to the left and right boundaries and vertices of the unit cell imposing the following constraints for the dependent variables: $u_{x=0} = u_{x=\lambda}$, $v_{x=0} = v_{x=\lambda}$, $V_{x=0} = V_{x=\lambda}$. After applying the boundary conditions, a frequency analysis is performed and the admittance of the resonator is computed with the relation:

$$Y(\omega) = \frac{J_{ns}}{V_0}, \tag{6}$$

where J_{ns} is the current in the electrode and ω is the angular frequency.

Table 1. Material constants used in the FEM simulation

Material	Au (IDT Electrodes)	GaN (Piezoelectric layer)	
ρ [kg/m^3]	19300	6150	
E [Pa]	79e9	–	
σ [S/m]	45.6e6	–	
ε_s	–	9	
Piezoel. constants e [Cm^{-2}]	–	e_{31}	–0.34
		e_{33}	0.67
		e_{15}	–0.3
Elastic constants c_E [GPa]	–	C_{11}	370
		C_{12}	145
		C_{13}	110
		C_{33}	390
		C_{44}	90

3.1. SAW structure A

The finger/interdigit width is 200 nm which corresponds to $\lambda = 0.8\,\mu m$ for the acoustic wave.

In this case, several simulations have been performed for different Silicon layer thicknesses: 10, 20, 40, 80, 400 μm and Table 2 summarizes the computation efforts registered during simulations. The simulation time is measured on a machine running 64 bits Windows with Intel Xeon CPU E5620 and 8 GB of RAM.

Table 2. Computation resources of FEM simulations for structure A

hSi [μm]	Mesh elements	Simulation time [s]	Resonance frequency [GHz]
10	3800	3316	5.472
20	5400	4371	5.472
40	8600	6559	5.472
80	15000	12201	5.472
400	66200	132538	5.472

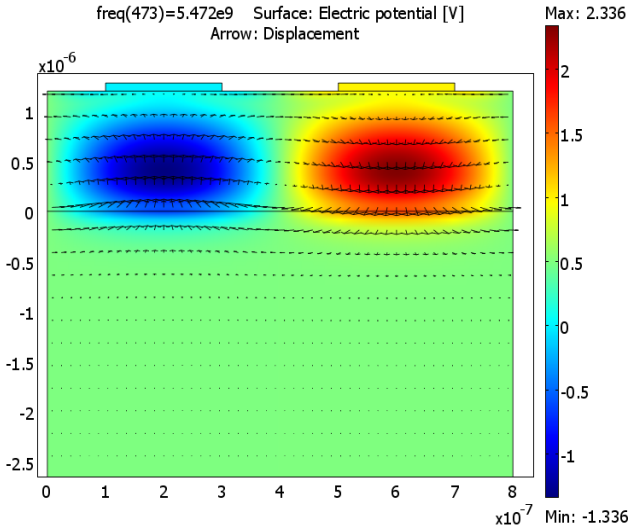

Fig. 2. Electric potential and total displacement (arrow) of SAW structure A at resonance frequency (5.472 GHz).

The mesh employed in the simulation is tetrahedral. The solution time and memory requirements are strongly related to the number of degrees of freedom (dofs) in the model. In case of 10 μm Si thickness the number of dofs is 46413 while for 400 μm Si thick is 799893. A higher mesh is applied to the electrodes and the domain is discretized to higher densities near the surface than near the bottom. No shift is observed in the resonance frequency with the increase of the Si thickness. In order to reduce the computation time in the first step of the design, the depth of the substrate has been chosen 10 μm. Two resonance frequencies have been observed: 5.472 GHz and 5.804 GHz. In order to choose the proper mode of propagation the electric field

and the electric potential variations have been checked in both cases and the second resonance behaves as a parasitic. The electric potential and total displacement at the resonance frequency 5.472 GHz are represented in Fig. 2 (zoomed on the area of interest). The displacements are in the order 10^{-9} m with the wavelength being 0.8 μm. Both the displacements and the electric potential die down within 2 to 3 wavelengths as seen from Fig. 4 and Fig. 5 which is typical of Rayleigh SAW propagation [20].

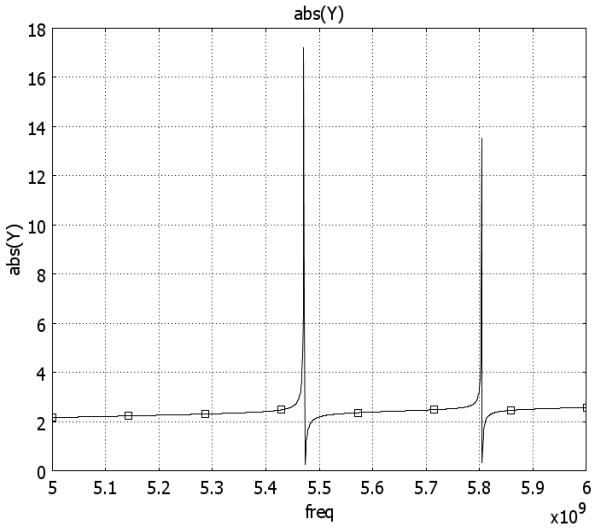

Fig. 3. Simulated admittance as a function of frequency for SAW structure A.

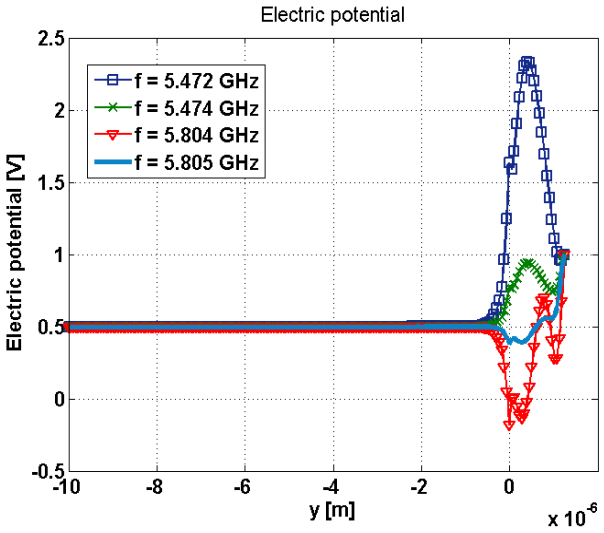

Fig. 4. Electric potential of SAW structure A at resonance (5.472 GHz, 5.804 GHz) and anti-resonant (5.474 GHz, 5.805 GHz) frequencies as a function of depth.

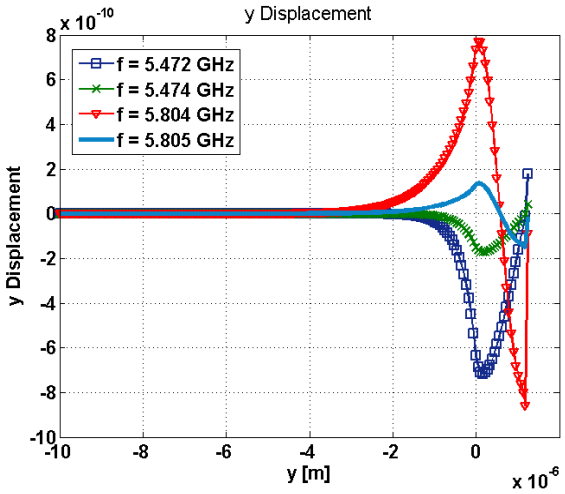

Fig. 5. y Displacement of SAW structure A at resonance (5.472 GHz, 5.804 GHz) and anti-resonant (5.474 GHz, 5.805 GHz) frequencies as a function of depth.

3.2. SAW structure B

In this case (Fig. 1 right) the electrode pitch is $\lambda = 1.6$ µm. The mesh consists in 7600 elements conducting to a system of 92553 dofs. The simulation time required for this example was 12743 s. Our experience showed that the mesh density slightly influences the central frequency. Figure 6 represents the admittance magnitude of structure B showing a resonance frequency at 2.79 GHz (Si thickness is 10 µm) corresponding to a lower acoustic velocity of 2232 m/s, compared to 4376 m/s obtained for single electrode transducer (case A).

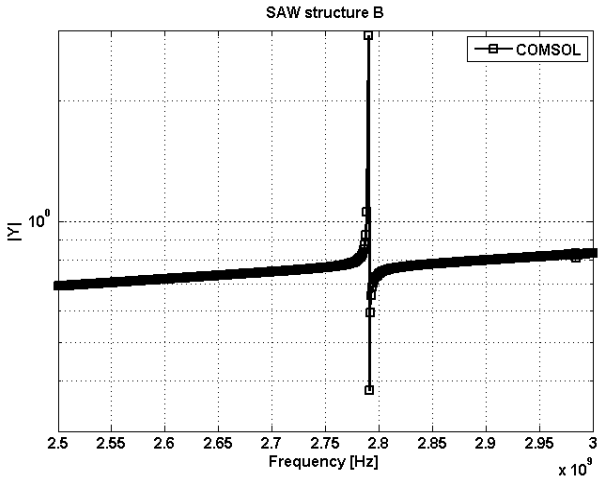

Fig. 6. Simulated admittance of test structure B.

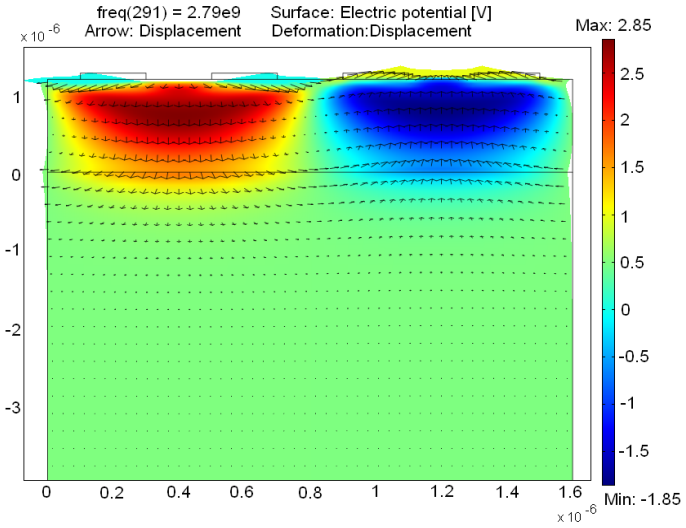

Fig. 7. Electric potential and total displacement (arrow) of SAW structure B at resonance frequency (2.79 GHz).

The electric potential of the structure and distortion of the material (arrows) are illustrated in Fig. 4. The electric potential inside the piezoelectric layer is higher (maximum value 2.85 V) than 1 V found on the electrodes. The maximum displacement of the material is 3.3 nm with the wavelength of 1.6 μm. The arrows show the behaviour of the waves generated on the surface of the structure.

4. Fabrication and characterization

The test structures consist in two SAW IDT structures placed face to face at 200 μm. The structures are fed by means of 50/100/50 μm coplanar waveguide transmission lines for "on-wafer" measurements. Both structures have 100 fingers, 100 interdigits and 60 reflectors. The fingers have a length of 274.6 μm. GaN/Si wafers grown on high-resistivity (111)-oriented silicon wafers, obtained on a commercial basis from NTT-AT, Japan, have been used. A buffer layer (composed by AlN and AlGaN) with a total thickness of 0.2 μm was grown between the silicon (400 μm thick) wafer and the 1 μm-thin undoped GaN top layer.

The first step in the SAW structure manufacturing was the patterning and deposition of the connection pads. For this, conventional photolithography, e-gun metallization (Ti/Au 20 nm/400 nm) and lift-off technique have been used. A direct Electron Beam Lithography (EBL) writing employing PMMA resist with a thickness of 200 nm was developed, for the IDT structure. Finally, a Ti/Au (5 nm/75 nm) layer was selectively deposited by e- gun evaporation and lift-off process. The excellent quality of the nano-lithographical process obtained using the "E-line" equipment from Raith GmbH, had as result a successful process, with a yield higher than 90%, using a single metal-PMMA layer structure.

SEM photos of the two types of SAW test structures with 200 nm wide fingers/interdigits on the IDT are presented in Fig. 8. The insets represent the schematics of the structures, including the pads.

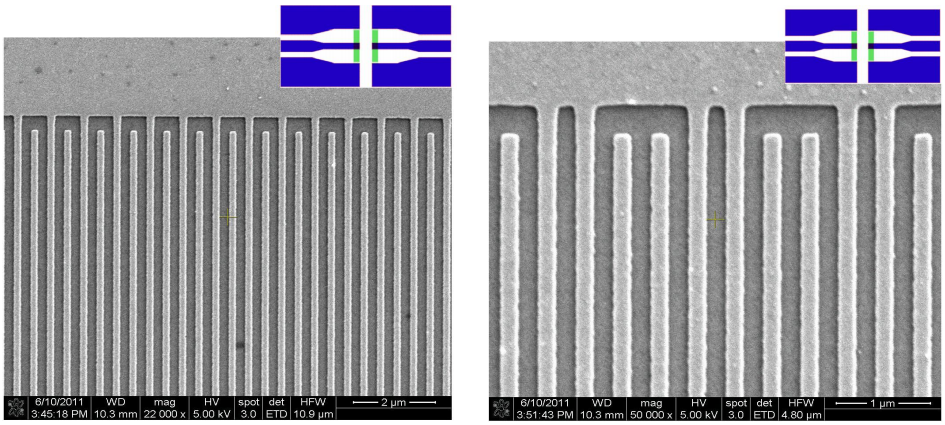

a) Test structure A – classic electrode transducer

b) Test structure B – split electrode transducer

Fig. 8. SEM photograph of the tests structure (IDT fingers 200 nm and distance between IDTs d = 200 µm). The inset presents a schematic of an entire structure, including the connection pads.

S parameters have been measured with a Vector Network Analyzer 37397D from Anritsu with a PM5 on wafer set-up from Suss Microtec, using the measuring pads of the structure (the inset of Fig. 5). In case of structure A, from the S_{11} characteristics, the resonance frequency of approximately 5.69 GHz is extracted, while for structure B, a resonance of 2.21 GHz is extracted. The resonance frequencies are in agreement with the simulations performed.

Transmission parameters S_{21} are presented in Fig. 9. Using this experimental data, the acoustic wave velocity between IDTs is extracted as 3.740 m/s, in very good agreement with that of 3.693 m/s, reported in [21] for GaN on sapphire.

5. Conclusions

A detailed Finite Element analysis was carried out for two types of SAW resonators to observe the piezoelectric effect and the frequency response. The structures have been fabricated and IDTs fingers and spacings of 200 nm wide have been obtained by e-beam lithography. A complete characterization of the structures has been performed. The transfer characteristics show a maximum transmission and a minimum reflection at 5.69 GHz for structure A and at 2.21 GHz for structure B. For a better prediction of the resonance frequencies through simulations, it is indicated to take into consideration the length of the resonator in a 3D modeling. The SAW structures investigated in this paper served only as test vehicles targeted to provide input in-

formation for the modeling and realization of more complex structures such as SAW temperature sensors or SAW filters.

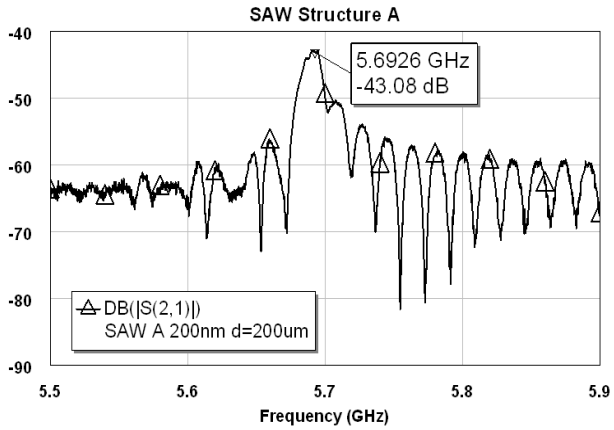

a) Transmission parameter (S_{21}) for SAW structure A

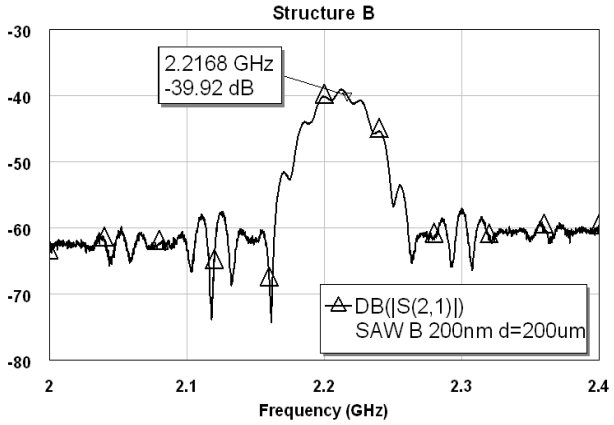

b) Transmission parameter (S_{21}) for SAW structure B

Fig. 9. Transmission measurements for the SAW test structure having a 200 μm distance between the IDTs.

Acknowledgements. The author Alexandra Ştefănescu acknowledges the support of the Sectoral Operational Program Human Resource Development (SOP HRD) financed from the European Social Fund and by the Romanian Government under the contract number POSDRU/89/1.5/S/63700.

References

[1] Zhang B., Zaghloul M. E., *Improved Surface Acoustic Wave Filter Design with Low Insertion Loss*, *53rd IEEE International Midwest Symposium on Circuits and Systems (MWSCAS)*, 2010.

[2] Hoang T., Rey P., Vaudaine M.- H., Robert P., Benech P., *Effect of Mo Layer on Performance of AlN/Si SAW Filter*, *Frequency Control Symposium, IEEE International*, 2008.

[3] El Gowini M. M., Moussa W. A., *A Finite Element Model of a MEMS-based Surface Acoustic Wave Hydrogen Sensor*, Sensors, **10**, pp. 1232–1250, 2010.

[4] Liu Y., Wang C. H., Li Y., *BCB film based SAW humidity sensor*, Electronics Letters, Vol. **47**, Issue 18, pp. 1012-1014, 2011.

[5] Petroni S., Tripoli G., Combi C., Vigna B., De Vittorio M., Todaro M. T., Epifani G., Cingolani R., Passaseo A., *Noise reduction in GaN-based radio frequency surface acoustic wave filters*, Applied Physics Letters, Vol. **85**, No. 6, pp. 1039–1041, 2004.

[6] Arslan E., Ozturk M. K., Teke A., Ozcelik S., Ozbay E., *Buffer optimization for crack-free GaN epitaxial layers grown on Si(111) substrate by MOCVD*, Journal of Physics D: Applied Physics, Vol. **41**, 155317, 2008.

[7] Feng Z. C., Zhang X., Chua S. J., Yang T. R., Dang J. C., Xu G., *Optical and structural properties of GaN materials and structures grown on Si by metalorganic chemical vapor deposition*, Thin Solid Films, Vol. **409**, Issue 1, pp. 15–22, 2002.

[8] Dadgar A., Veit P., Schulze F., Bläsing J., Krtschil A., Witte H., Diez A., Hempel T., Christen J., Clos R., Krost A., *MOVPE growth of GaN on Si – Substrates and strain*, Thin Solid Films, Vol. **515**, Issue 10, pp. 4356–4361, 2007.

[9] Müller A., Neculoiu D., Konstantinidis G., Deligeorgis G., Dinescu A., Stavrinidis A., Cismaru A., Dragoman M., Stefanescu A., *SAW Devices Manufactured on GaN/Si for Frequencies Beyond 5 GHz*, IEEE Electron Device Letters, Vol. **31**, No. 12, 2010.

[10] Peng D., Yu T., Yu F., *Boundary Conditions for Simulating Large SAW Device Using ANSYS*, IEEE Transactions on Ultrasonics, Ferroelectrics and Frequency Control, Vol. **57**, No. 8, 2010.

[11] Zhgoon S., Tsimbal D., Shvetsov A., Bhattacharjee K., *3D Finite Element Modeling of Real Size SAW Devices and Experimental Validation*, *IEEE Ultrasonics Symposium*, IUS 2008.

[12] Chung G.-S., Phan D.-T., *Finite Element Modeling of Surface Acoustic Waves in Piezoelectric Thin Films*, Journal of Korean Physical Society, Vol. **57**, No. 3, 2010.

[13] Stefanescu A., Müller A., Dinescu A., Konstantinidis G., Cismaru A., Stavrinidis A., Neculoiu D., *FEM Analysis of GaN Based Surface Acoustic Wave Resonators*, *Proceedings International Semiconductor Conference (CAS 2011)*, Vol. **1**, pp. 177–180, 2011.

[14] Hofer M., Finger N., Kovacs G., Schoberl J., Zaglmayr S., Langer U., Lerch R., *Finite Element Simulation of Wave Propagation in Periodic Piezoelectric SAW Structures*, IEEE Transactions on Ultrasonics, Ferroelectrics and Frequency Control, Vol. **53**, Issue 6, 2000.

[15] Yong Y.-K., *Analysis of Periodic Structures for BAW and SAW Resonators*, IEEE Ultrasonics Symposium, Vol. **1**, pp. 781–790, 2001.

[16] Morgan D., *Surface Acoustic Filters with applications to electronic communications and signal processing*, Elsevier, UK, 2007.

[17] Tigli O., Zaghloul M. E., *A Novel SAW Device in CMOS: Design, Modeling and Fabrication*, IEEE Sensors Journal, Vol. **7**, No. 2, 2007.

[18] COMSOL webpage, `www.comsol.com`

[19] Available online: `http://www.ioffe.ru/SVA/NSM/Semicond/GaN/basic.html`

[20] Kannan T., *Finite Element Analysis of Surface Acoustic Wave Resonators*, Master of Science Thesis, University of Saskatchewan, 2006.

[21] Palacios T., Calle F., Grajal J., Monroy E., Eickhoff M., Ambacher O., Omnes F., *High frequency SAW devices on AlGaN: Fabrication, characterization and integration with optoelectronics*, *Proceedings IEEE Ultrasonics Symposium*, pp. 57–60, 2002.